NANO LETTERS

2009
Vol. 9, No. 6
2384-2389

Nanostructured Gold Films for SERS by Block Copolymer-Templated Galvanic Displacement Reactions

Yong Wang,*,†,‡ Michael Becker,†,§ Li Wang,† Jinquan Liu,† Roland Scholz,† Juan Peng,|| Ulrich Gösele,† Silke Christiansen,†,§ Dong Ha Kim,*,⊥ and Martin Steinhart*,†,#

Max Planck Institute of Microstructure Physics, Weinberg 2, D-06120 Halle, Germany, State Key Laboratory of Materials-Oriented Chemical Engineering, College of Chemistry and Chemical Engineering, Nanjing University of Technology, Nanjing 210009, Jiangsu, People's Republic of China, Institute of Photonic Technology, Albert-Einstein-Str. 9, 07745 Jena, Germany, The Key Laboratory of Molecular Engineering of Polymers, Ministry of Education, Department of Macromolecular Science, Fudan University, Shanghai 200433, China, Department of Chemistry and Nano Science, Ewha Womans University, 11-1 Daehyun-Dong, Seodaemun-Gu, Seoul 120-750, Korea, and Institute for Chemistry, University of Osnabrück, Osnabrück, Germany

Received March 25, 2009; Revised Manuscript Received May 9, 2009

ABSTRACT

Up to now, little effort has been made to exploit large-area high-throughput patterning by block copolymer (BCP) lithography to generate nanostructured substrates with periods well below 100 nm for surface-enhanced Raman scattering (SERS). We show that simple BCP-templated galvanic displacement reactions yield dense arrays of mushroom-shaped gold nanopillars with a period of 50 nm. The nanoporous BCP films used as templates were obtained by swelling-induced reconstruction of reverse micelle monolayers deposited on silicon wafers. Coupling of adjacent mushroom caps almost impinging on each other combined with their strong local curvature results in a high spatial density of hot spots in the narrow gaps between them. Thus, substrates characterized by high SERS efficiencies are obtained.

Surface-enhanced Raman scattering (SERS)[1−3] has been explored as a powerful high-throughput technique for trace analysis and in situ monitoring of molecular processes. SERS is based on the field enhancement related to surface plasmons at the surfaces of metal substrates with plasmon resonances lying in the visible spectral range. Probe molecules attached to substrates consisting of SERS-active metals, such as silver and gold, exhibit dramatically enhanced Raman scattering intensities and therefore can be detected with likewise dramatically enhanced sensitivity. Particularly attractive configurations for SERS-active systems are based on metal nanoparticles,[4−8] the size and shape of which influence their SERS performance to a large extent.[9] On the one hand, strong local electromagnetic field enhancement accompanied by significantly enhanced Raman scattering occurs at edges and corners of nanoparticles too small to allow for multipolar excitations.[10,11] While polyhedral metal nanoparticles can be produced by a variety of synthetic approaches,[12−14] it is understood that only the presence of sharp protrusions and crevices leads to this effect.[15] On the other hand, it was predicted[10,15,16] and experimentally shown[17,18] that highly localized plasmon modes created by strong electromagnetic coupling between almost or even slightly touching metallic objects result in the formation of small volumes characterized by strongly enhanced electromagnetic fields, which are referred to as "hot spots". SERS intensities originating from analytes located at such hot spots may exceed those of identical analytes attached to isolated nanoparticles by several orders of magnitude.

Serial and parallel top-down patterning techniques, such as electron beam lithography,[19] optical lithography, and nanoimprint lithography, were employed to fabricate SERS substrates but are associated with limitations regarding either throughput and patternable area or processable materials and realizable array geometries. Bottom-up approaches for the production of SERS substrates have included nanosphere

* To whom correspondence should be addressed. E-mail: (Y.W.) yongwang@njut.edu.cn; (D.H.K.) dhkim@ewha.ac.kr; (M.S.) martin.steinhart@uos.de.
† Max Planck Institute of Microstructure Physics.
‡ Nanjing University of Technology.
§ Institute of Photonic Technology.
|| Fudan University.
⊥ Ewha Womans University.
University of Osnabrück.

10.1021/nl900939y CCC: $40.75
Published on Web 05/21/2009

lithography[20] and the self-assembly of colloidal Au and Ag nanoparticles.[21] However, the patterns accessible by nanosphere lithography have characteristic length scales of a few 100 nm and above, thus exceeding the dimensions ideal for SERS by 1 order of magnitude, and colloidal metal nanoparticles are difficult to assemble into dense and extended two-dimensional layers if they have diameters in the sub-100 nm range or if they have nonspherical shapes. Only little effort has been made to use block copolymers (BCPs)[22−24] as templates in the preparation of SERS substrates, even though their characteristic periods match the length scales required for efficient SERS. Russell and co-workers treated a BCP containing inorganic polyferrocenylsilane blocks with oxygen plasma to generate arrays of nanoscopic iron-containing silicon oxide dots. The substrate thus patterned by BCP self-assembly was sputter-coated with a silver film, the SERS efficiency of which was studied.[25]

It has remained challenging to meet the design criteria for highly efficient and durable SERS-active systems, which would ideally be configured as dense, two-dimensional assemblies of metal nanostructures with periods and feature sizes well below 100 nm. Central to high SERS performance is the maximization of the spatial density of hot spots. To this end, the metal nanostructures should have strongly curved edges or protrusions separated by very narrow gaps or even impinging on each other. Here we show that a simple BCP-templated galvanic displacement reaction[26,27] that involves neither high-temperature treatments nor dry etching steps allows reliably producing SERS substrates with periods in the 50 nm range at high throughput. Thus, arrays of mushroom-shaped gold nanostructures touching or almost touching their nearest neighbors are obtained that show significantly higher Raman scattering enhancement than arrays of separated gold nanopillars formed at shorter reaction times, apparently because interactions between adjacent mushroom caps create a large number of hot spots.

The BCP-templated formation of arrays of gold nanostructures for SERS is schematically summarized in Scheme 1. We used asymmetric polystyrene-*block*-poly(2-vinylpyridine) (PS-*b*-P2VP; M_n (PS) = 50000 g/mol, M_n (P2VP) = 16500 g/mol, M_w/M_n = 1.09, Polymer Source Inc.) as BCP template that forms reverse micelles consisting of a swollen PS corona and a condensed P2VP core in nonpolar solvents selective to PS. Following procedures described elsewhere,[28] we spin-coated a 0.5 wt % solution of PS-*b*-P2VP in toluene at 2000 rpm onto n-type (100) Si wafers.[29] Thus, a hexagonal monolayer of reverse PS-*b*-P2VP micelles with a period of 50 nm, as determined by atomic force microscopy, was obtained. Preferential interaction and swelling of the minor component of an asymmetric BCP in a thin-film configuration with a selective solvent can lead to a reconstruction of the film morphology. In such a reconstruction process, the minor component segregates to the surfaces and surrounds a scaffold of the major component. At the initial positions of minor-component domains, nanopores oriented normal to the film plane penetrating through the entire film form.[30] We applied a procedure introduced by Li et al. to convert the reverse PS-*b*-P2VP micelle monolayers into nanoporous

Scheme 1. Fabrication of Nanostructured Gold Substrates for SERS by BCP-Templated Galvanic Displacement (PS, Blue; P2VP, Orange; Si, Black; Au, Yellow)[a]

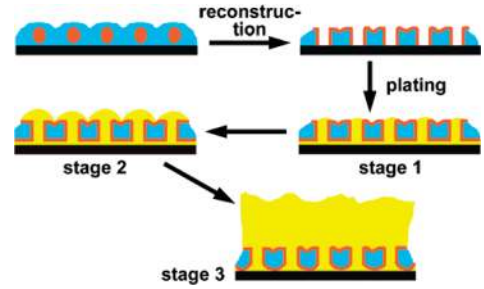

[a] A monolayer of inverse PS-*b*-P2VP micelles is deposited on a Si wafer by spin coating (top left). Morphology reconstruction by treatment with acetic acid leads to the formation of a nanoporous BCP template (top right). Exposure to a $NaAuCl_4$/HF plating solution yields at first an array of Au nanopillars connected to a continuous Au film on the Si wafer (stage 1 of the plating process). Caps grow on top of the Au nanopillars as soon as they completely fill the nanopores in the BCP template (stage 2). Upon further deposition of gold, the order imposed by the BCP template deteriorates, and eventually a thick gold film with surface features characterized by length scales similar to those accessible by top-down lithography and self-assembly of colloids results (stage 3).

films.[28] Exposure to acetic acid, a selective solvent for the minor component P2VP, for 5 min resulted in the segregation of P2VP to the surfaces and the walls of the nanopores formed at the positions of the P2VP domains, whereas the glassy PS matrix stabilized the initial hexagonal order of the BCP template.

Galvanic displacement reactions occur if solid semiconductors are exposed to aqueous plating solutions and involve spontaneous reduction of metal ions on the surface of the semiconductor, resulting in the deposition of the metal. This cathodic process is accompanied by an anodic process leading to oxidative dissolution of the semiconductor.[31] It was shown that gold is deposited on Si surfaces from solutions containing tetrachloroaurate $[AuCl_4]^-$ and hydrofluoric acid (HF) accompanied by partial dissolution of Si and the formation of $[SiF_6]^{2-}$.[32] To deposit gold, we adapted the type of galvanic displacement reaction referred to as "method 2" in refs 26 and 27. Thus, we exposed silicon wafers coated with nanoporous PS-*b*-P2VP films obtained by reconstruction of reverse micelle monolayers to an aqueous solution of 20 mL 0.02 M $NaAuCl_4$ in 18 mL 49% HF for various plating times t_p. After the removal of the samples from the plating solution, the PS-*b*-P2VP was extracted by treatment with tetrahydrofuran. A first analysis of the surface structure of the SERS substrates thus obtained was carried out by scanning electron microscopy (SEM).[33] For a more detailed investigation of the structure evolution in the course of the galvanic displacement process by transmission electron microscopy (TEM), we prepared cross-sectional specimens by slicing the samples perpendicular to the surfaces of the Si wafers.[34]

We identified three different stages of the galvanic displacement process by the structural characterization of gold layers obtained after different plating times. A plating time of 15 s yielded a nanostructured gold film with a morphology corresponding to stage 1. Gold nanopillars with diameters of about 30 nm arranged in an array with a period of ≈50 nm, corresponding to that of the BCP template, are

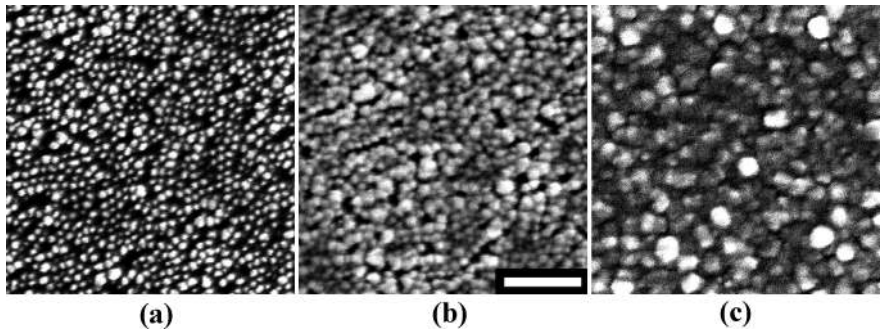

Figure 1. SEM top view images of nanostructured gold films on Si wafers obtained by BCP-templated galvanic displacement reactions. (a) Stage 1 sample obtained by plating for 15 s; (b) stage 2 sample obtained by plating for 30 s; (c) stage 3 sample obtained by plating for 90 s. The micrographs have the same magnification. The scale bar in (b) corresponds to 300 nm.

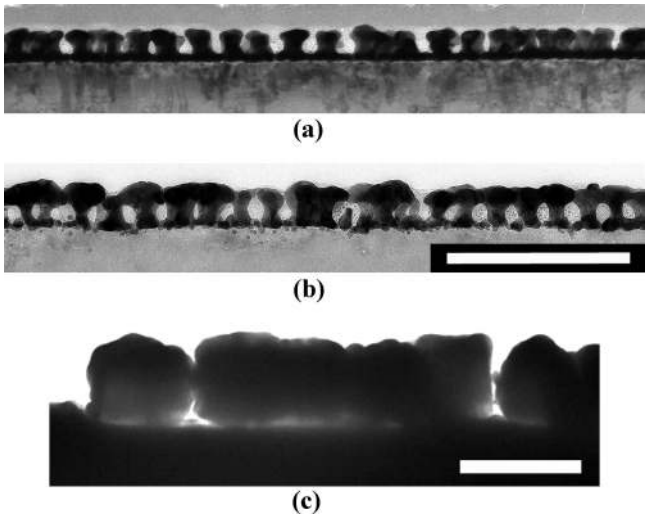

Figure 2. TEM images of cross-sectional specimens cut normal to the surface of the Si wafers. (a) Stage 1 sample obtained by plating for 15 s; (b) stage 2 sample obtained by plating for 30 s; (c) stage 3 sample obtained by plating for 90 s. Panels (a) and (b) have the same magnification. The scale bar in (b) corresponds to 200 nm and that in (c) to 1 μm. In (a) and (b), the Au in the middle appears darker than the underlying Si wafer at the bottom. In (c), the bright region separating the Au layer in the middle and the Si wafer at the bottom denotes the volume in which the BCP templated gold deposition. Note the step edge on the left that indicates that a significant amount of Si had been dissolved.

seen in Figure 1a, which is an SEM top view image. The gold nanopillar array apparently mimics the BCP template, that is, the nanopillars formed at the position of the nanopores in the reconstructed reverse PS-*b*-P2VP micelle monolayer. As obvious from the cross-sectional TEM image shown in Figure 2a, the nanopillars, which were connected with an underlying, continuous gold film with a thickness of ~8 nm, had a slightly waisted shape. The diameter of their central section amounts to ~18 nm, and their height of ~27 nm was uniform over the entire array. We assume that during plating not only the pore walls of the BCP template but also a layer between the glassy PS domains and the surface of the Si wafer consist of P2VP. Given the high affinity of $[AuCl_4]^-$ to P2VP and the partial dissolution of the Si, $[AuCl_4]^-$ anions could access not only the pores in the BCP template but also the area below the PS domains. Hence, a continuous Au film forms on the surface of the Si wafer. However, migration of the $[AuCl_4]^-$ anions into the space below the PS is increasingly hampered as gold nanopillars grow in the nanopores of the BCP template. Therefore, after some time Au exclusively precipitates at the tips of the nanopillars, and an array of gold nanopillars connected to an underlying continuous gold film is thus obtained in stage 1 of the plating process.

After plating for 30 s, the second stage of the plating process becomes evident. Once the nanopores of the BCP template are completely filled with gold, the BCP scaffold no longer laterally confines the cathodic deposition of the metal. Thus, mushroom-shaped entities form by the growth of caps on top of the nanopillars, which impinge on each other when their diameter approaches the period of the BCP template (Figures 1b and 2b). A regular array of stems connects the caps with the Si wafer. The mushroom layer is significantly thicker (~50 nm) than the ~35 nm thick stage one-gold layer (nanopillars and underlying Au film) obtained at $t_p = 15$ s. Eventually, the third stage of the plating process is reached when the mushroom caps merge into a thick gold layer on top of the BCP template and the order imposed by the BCP template deteriorates upon further deposition of gold. For example, the SEM top view image of a gold layer obtained by plating for 90 s shows features with characteristic lengths well above 150 nm (Figure 1c), hence significantly exceeding the period of the BCP template but corresponding to the length scales typically accessible by top-down lithography and self-assembly of colloids. The cross-sectional TEM image of the 90 s sample reveals that the gold layer is 700−800 nm thick, whereas the peak-to-valley distances of the surface features are of the order of 100 nm and above (Figure 1c). Note the bright stripe separating the deposited gold on the top and the silicon wafer at the bottom, which denotes the layer in which the galvanic displacement reaction was templated by the BCP, and the surface profile of the Si wafer. Especially from the step edge on the left, it is obvious that a significant amount of Si corresponding to a layer thickness of a few 100 nm was dissolved in the course of the galvanic displacement process.

To evaluate their performance, the SERS substrates obtained after various plating times were cleaned with acetone and water, exposed to 10^{-5} molar aqueous crystal violet (CV) solution for 10 min and then rinsed with

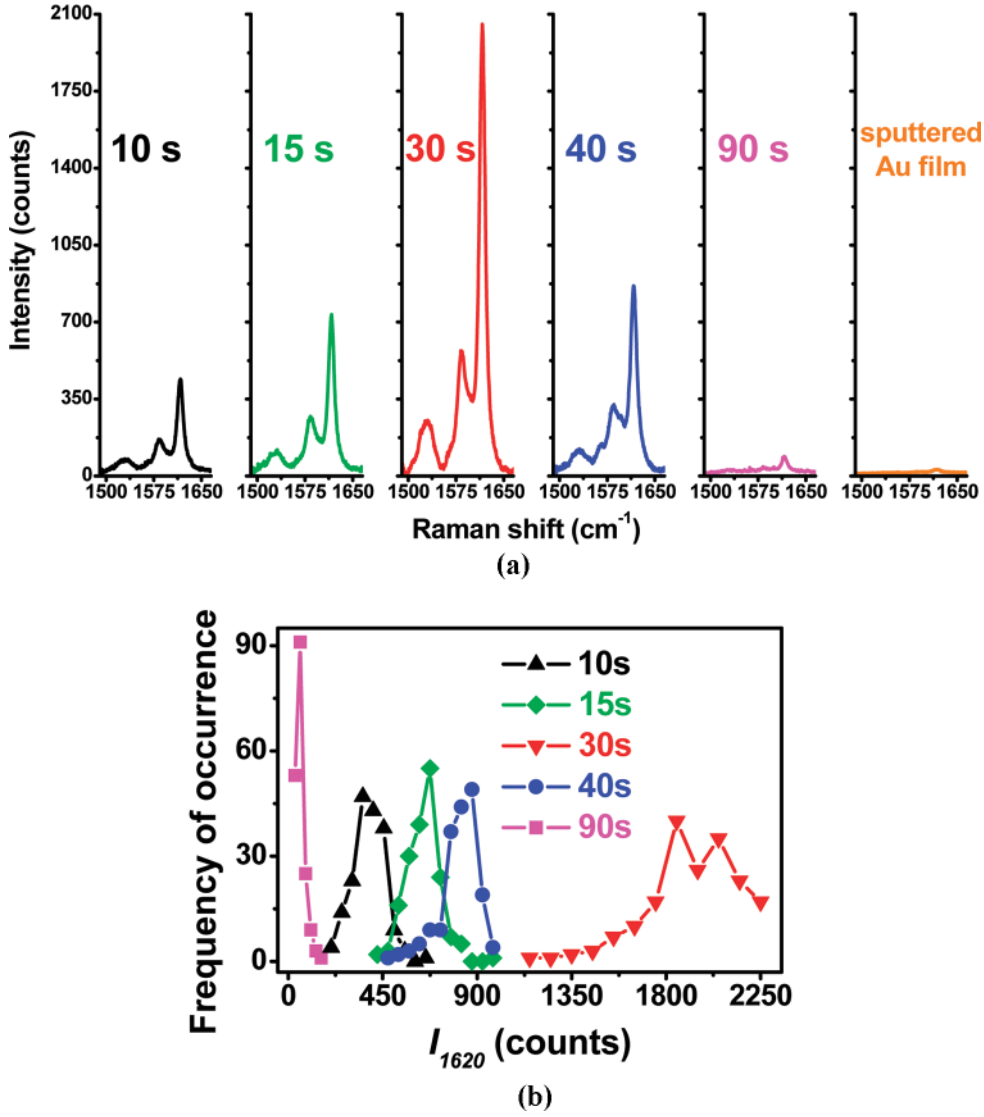

Figure 3. Evaluation of the SERS performance of gold substrates obtained by BCP-templated galvanic displacement reactions (plating times 10, 15, 30, 40, and 90 s) after exposure to a 10^{-5} molar aqueous solution of crystal violet for 10 min. (a) Average of 182 spectra acquired at 182 spots arranged in a matrix of 13 × 14 spots covering an area of 18.2 μm × 19.9 μm. For comparison, an averaged spectrum of a sputtered gold film on a Si wafer obtained in the same way is also shown. (b) Distributions of the frequencies of occurrence of peak heights I_{1620} at a Raman shift of 1620 cm^{-1} in the 182 spectra measured per sample.

deionized water. SERS measurements were carried out in reflection using a Horiba Jobin Yvon LabRAM HR 800 high-resolution Raman microscope configured with a thermoelectrically cooled CCD array detector and a HeNe laser emitting at 633 nm with an intensity of 6.4 mW. The laser beam was focused on the surface of the samples, where the laser intensity was reduced to 0.45 mW. The laser spot on the sample surface had a diameter of ~3 μm and covered about 3265 elements of the hexagonal lattice initially defined by the BCP template. The SERS spectra thus obtained were analyzed with the program LabSpec. On each sample, for a matrix of 13 × 14 = 182 spots covering an area of 18.2 μm × 19.9 μm two spectra per spot were acquired (acquisition time 2 × 30 s), averaged and background-corrected using a parabolic function. Figure 3a displays the averages of the 182 processed SERS spectra obtained per sample. The SERS spectrum of CV contains three characteristic peaks ascribed to ring C−C stretching modes, the most intense of which appears at a Raman shift of about 1620 cm^{-1}.[35,36] We compared the height I_{1620} of the latter peak in order to rank the samples according to their SERS efficiency. Stage 1 SERS substrates already show a significant SERS effect. Plating for 10 s resulted in an I_{1620} value of 440 counts, which increased to about 730 counts for t_p = 15 s (Figures 1a and 2a). The by far strongest SERS efficiency, as evidenced by the outstandingly high I_{1620} value of 2054 counts, was found for the stage 2 sample fabricated by plating for 30 s seen in Figures 1b and 2b. Dense arrays of entities having a mushroomlike shape can be considered as nearly ideal SERS substrates characterized by high spatial density of easily accessible hot spots. These hot spots occur where the gaps between the sharp edges of adjacent mushrooms caps have widths corresponding to molecular length scales. Then, a combination of strong local curvature and interactions between neighboring metal nanostructures cause extraordinarily high local field enhancement. Plating for 40 s led to

a decrease in I_{1620}, which amounted to 870 counts, apparently because hot spots vanish upon further deposition of gold. Eventually, the stage 3 sample obtained by plating for 90 s showed, as compared to stage 1 and stage 2 samples, only a relatively weak SERS effect, and I_{1620} decreased to 90 counts.

Quantifying the absolute enhancement factor G of rough nanostructured SERS substrates is still a matter of debate[37] and requires plausible assumptions regarding the surface density of adsorbed dye molecules. G can be defined as[37,38]

$$G = \frac{I_{1620,\mathrm{surf}}/N_{\mathrm{surf}}}{I_{1620,\mathrm{bulk}}/N_{\mathrm{bulk}}}$$

where $I_{1620,\mathrm{surf}}$ denotes I_{1620} in the SERS spectra, and $I_{1620,\mathrm{bulk}}$ the corresponding I_{1620} values in Raman spectra measured in the absence of enhancement. N_{surf} and N_{bulk} are the numbers of effectively excited molecules. Following the method reported by Cai et al.,[38] we determined $I_{1620,\mathrm{bulk}}$ and obtained an intensity per CV molecule in the effective excitation volume of $\sim 5.71 \times 10^{-6}$ counts.[39] On the stage 1 sample ($t_p = 15$ s) and the stage 2 sample ($t_p = 30$ s), 0.02 mL of the 10^{-5} molar aqueous CV solution were spread. Since we used wafer pieces with an area of 40 mm^2, 2129 CV molecules were located within the laser spot during the acquisition of the SERS spectra, assuming that 10% of the CV molecules initially present in the applied aliquot of the CV solution were adsorbed on the sample surface and contributed equally to the detected SERS signal. Thus, for the stage 2 sample ($t_p = 30$ s), G would amount to about 1.7×10^5. However, it is reasonable to assume that the number of CV molecules actually remaining on the sample surface after washing off the CV solution is much smaller. If only one percent of the molecules were adsorbed, an enhancement factor of about 1.7×10^6 would result. Therefore, we consider 1.7×10^5 as a reasonable lower limit for the actual enhancement.

We compared the SERS spectrum of the stage 2 sample ($t_p = 30$ s) to that of a gold layer sputtered on a Si wafer[40] to estimate the relative enhancement caused by the topography of the mushroom array. The I_{1620} value apparent in the averaged spectrum of the stage 2 sample ($t_p = 30$ s) is about 256 times larger than that seen in the averaged spectrum of the sputtered Au film. In the latter case, I_{1620} amounts to about 8 counts (Figure 3a). A 4-fold increase in I_{1620} can be ascribed to differences in the areas of the gold surfaces in the laser spot of the Raman microscope. The effective area of the gold surface of the stage 2 sample ($t_p = 30$ s) in the laser spot is four times larger than that of the sputtered Au layer. However, the additional enhancement of I_{1620} by a factor of about 64 must be related to the presence of hot spots in the mushroom array.

Distributions of the frequencies of occurrence of the peak heights at 1620 cm^{-1}, which are indicative of the spatial homogeneity of SERS across the substrates, are shown in Figure 3b. The gold nanostructure arrays formed in the initial phase of the BCP-templated galvanic displacement process are characterized by high spatial uniformity, as obvious from the narrow peak height distributions belonging to the stage 1 samples ($t_p = 10$ s; $t_p = 15$ s), which have full widths at half-maximum (fwhm) values of about 150 counts. A broad peak height distribution was obtained for the stage 2 sample prepared by plating for 30 s. The deteriorated homogeneity of this sample reflects the occurrence of structural irregularities, which evolve as lateral confinement imposed by the BCP template is absent during the growth of the mushroom caps. The I_{1620} values of a small number of spots lie significantly below average but are still larger than any I_{1620} value of the other samples. The peak height distribution of the sample obtained by plating for 40 s is shifted to smaller I_{1620} values while it gets narrower (fwhm $\approx$ 160 counts). This outcome is in line with the assumption that, upon further deposition of gold into the interstices of the mushroom caps, hot spots are erased. Finally, the stage 3 sample obtained by plating for 90 s shows again a narrow peak height distribution at low I_{1620} values, mainly because hot spots yielding high SERS intensities are completely absent.

In conclusion, a combination of BCP lithography and a simple galvanic displacement reaction was exploited to prepare nanostructured gold films for SERS. In the first stage of the plating process, arrays of gold nanopillars connected to underlying continuous gold films formed, which were replicas of the nanoporous BCP templates. In the second stage, caps grew on top of the gold nanopillars once the nanopores of the BCP templates were completely filled. The high spatial density of hot spots located at narrow gaps between the sharp edges of adjacent mushrooms caps, where strong curvature and interparticle coupling caused strong field enhancement, resulted in a high SERS performance significantly exceeding that of sputtered gold layers. Thus, high-throughput and large-area patterning by BCP lithography can be exploited to generate high-performance SERS substrates with periods of a few tens of nanometers consisting of dense arrays of metal nanostructures with shapes and spacings optimized for high SERS performance.

Acknowledgment. Technical assistance by K. Sklarek and S. Hopfe is gratefully acknowledged, as well as financial support by the German Research Foundation (STE 1127/8-1; STE 1127/6-3; CH159/6-1), by the Max Planck Society (NanoSTRESS), and Korean Science and Engineering Foundation (KOSEF) funded by the Korean government (MEST) (No. R11-2005-008-00000-0). Y.W. thanks the Alexander von Humboldt Foundation for a fellowship.

References

(1) Fleischman, M.; Hendra, P. J.; McQuillan, A. J. *Chem. Phys. Lett.* **1974**, *26*, 163.
(2) Jeanmaire, D. L.; Van Duyne, R. P. *J. Electroanal. Chem.* **1977**, *84*, 1.
(3) Albrecht, M. G.; Creighton, J. A. *J. Am. Chem. Soc.* **1977**, *99*, 5215.
(4) Haynes, C.; McFarland, A.; Van Duyne, R. *Anal. Chem.* **2005**, *77*, 338.
(5) Baker, G. A.; Moore, D. S. *Anal. Bioanal. Chem.* **2005**, *382*, 1751.
(6) Banholzer, M. J.; Millstone, J. E.; Qin, L.; Mirkin, C. A. *Chem. Soc. Rev.* **2008**, *37*, 885.
(7) Brown, R. J. C.; Milton, M. J. T. *J. Raman Spectrosc.* **2008**, *39*, 1313.
(8) Ko, H.; Singamaneni, S.; Tsukruk, V. V. *Small* **2008**, *4*, 1576.
(9) Kelly, K. L.; Coronado, E.; Zhao, L. L.; Schatz, G. C. *J. Phys. Chem. B* **2003**, *107*, 668.
(10) Hao, E.; Schatz, G. C. *J. Chem. Phys.* **2004**, *120*, 357.

(11) Rang, M.; Jones, A. C.; Zhou, F.; Li, Z.-Y.; Wiley, B. J.; Xia, Y. N.; Raschke, M. B. *Nano Lett.* **2008**, *8*, 3357.
(12) Zhang, J.; Gao, Y.; Alvarez-Puebla, R. A.; Buriak, J. M.; Fenniri, H. *Adv. Mater.* **2006**, *18*, 3233.
(13) Tao, A. R.; Habas, S.; Yang, P. D. *Small* **2008**, *4*, 310.
(14) Xia, Y. N.; Xiong, Y.; Lim, B.; Skrabalak, S. E. *Angew. Chem., Int. Ed.* **2009**, *48*, 60.
(15) Xu, H.; Aizpurua, J.; Käll, M.; Apell, P. *Phys. Rev. E* **2000**, *62*, 4318.
(16) García-Vidal, F. J.; Pendry, J. B. *Phys. Rev. Lett.* **1996**, *77*, 1163.
(17) Xu, H.; Bjerneld, E. J.; Käll, M.; Börjesson, L. *Phys. Rev. Lett.* **1999**, *83*, 4357.
(18) Michaels, A. M.; Jiang, J.; Brus, L. *J. Phys. Chem. B* **2000**, *104*, 11965.
(19) Cialla, D.; Hübner, U.; Schneidewind, H.; Möller, R.; Popp, J. *ChemPhysChem* **2008**, *9*, 758.
(20) Camden, J. P.; Dieringer, J. A.; Zhao, J.; Van Duyne, R. P. *Acc. Chem. Res.* **2008**, *41*, 1653.
(21) Griffith Freeman, R.; Grabar, K. C.; Allison, K. J.; Bright, R. M.; Davis, J. A.; Guthrie, A. P.; Hommer, M. B.; Jackson, M. A.; Smith, P. C.; Walter, D. G.; Natan, M. J. *Science* **1995**, *267*, 1629.
(22) Spatz, J. P.; Mössmer, S.; Möller, M. *Chem.—Eur. J.* **1996**, *2*, 1552.
(23) Förster, S.; Antonietti, M. *Adv. Mater.* **1998**, *10*, 195.
(24) Park, C.; Yoon, J; Thomas, E. L. *Polymer* **2003**, *44*, 6725.
(25) Lu, J.; Chamberlin, D.; Rider, D. A.; Liu, M.; Manners, I.; Russell, T. P. *Nanotechnology* **2006**, *17*, 5792.
(26) Aizawa, M.; Buriak, J. M. *J. Am. Chem. Soc.* **2005**, *127*, 8932.
(27) Aizawa, M.; Buriak, J. M. *Chem. Mater.* **2007**, *19*, 5090.
(28) Li, X.; Tian, S. J.; Ping, Y.; Kim, D. H.; Knoll, W. *Langmuir* **2005**, *21*, 9393.
(29) The Si wafers (SI-MAT, Germany; resistivity according to the manufacturer: 0.01−0.02 Ω cm) were cleaned in a solution of 98% H_2SO_4 and 30% H_2O_2 (70/30 v/v) at 80°C for 30 minutes. After rinsing with deonized water and drying with nitrogen gas, the wafers were immersed into 5% HF for 5 s prior to the deposition of the micelle monolayer.
(30) Xu, T.; Stevens, J.; Villa, J. A.; Goldbach, J. T.; Guarini, K. W.; Black, C. T.; Hawker, C. J.; Russell, T. P. *Adv. Funct. Mater.* **2003**, *13*, 698.
(31) D'Asaro, L. A.; Nakahara, S.; Okinaka, Y. *J. Electrochem. Soc.* **1980**, *127*, 1935.
(32) Nagahara, L. A.; Ohmori, T.; Hashimoto, K.; Fujishima, K. J. *Vac. Sci. Technol., A* **1993**, *11*, 763.
(33) We used a JEOL JSM 6340F scanning electron microscope operated at 8 kV.
(34) Cross-sectional specimens were prepared by embedding the samples in epoxy resin and slicing them normal to the wafer surface with a diamond wire saw. The ∼400 μm thick sections thus obtained were ground, polished to a thickness of ∼80 μm, dimple-ground, further polished to a thickness of less than 15 μm and thinned to electron transparency by ion-milling from both sides with Ar (PIPS, Gatan). TEM investigations were performed with a Phillips CM20T operated at 200 kV.
(35) Schneider, S.; Brehm, G.; Freunscht, P. *Phys. Status Solidi B* **1995**, *189*, 37.
(36) Liang, E. J.; Ye, X. L.; Kiefer, W. *J. Phys. Chem. A* **1997**, *101*, 7330.
(37) Le Ru, E. C.; Blackie, E.; Meyer, M.; Etchegoin, P. G. *J. Phys. Chem. C* **2007**, *111*, 13794.
(38) Cai, W. B.; Ren, B.; Li, X. Q.; She, C. X.; Liu, F. M.; Cai, X. W.; Tian, Z. Q. *Surf. Sci.* **1998**, *406*, 9.
(39) Four Raman spectra of a 10^{-4} molar aqueous CV solution were measured applying a laser intensity of 6.4 mW and then averaged. The height of the peak at 1620 cm^{-1}, which amounted to 852 counts, was divided by 14.22, the ratio of the laser intensities applied to acquire the Raman and the SERS spectra, respectively. Thus, a corrected peak height of 60 counts was obtained. The effective excitation volume in solution of 174.6 μm^3 was derived using the method described in ref 38, and the number of molecules located within the effective excitation volume was calculated to be about 10 500 000.
(40) Au was sputtered onto the smooth surface of a Si wafer for 16 seconds (400 W, direct current) using a Discovery-18 sputter coater (Denton Vacuum). The nominal layer thickness was 20 nm.

NL900939Y